The Relative Importance of Aerosol Scattering and Absorption in Remote Sensing

ROBERT S. FRASER AND YORAM J. KAUFMAN

Abstract—**Previous attempts to explain the effect of aerosols on satellite measurements of surface properties for the visible and near-infrared spectrum have emphasized the amount of aerosols without consideration of their absorption properties. In order to estimate the importance of absorption, the radiances of the sunlight scattered from models of the Earth-atmosphere system are computed as functions of the aerosol optical thickness and absorption. The absorption effect is small where the surface reflectance is weak, but is important for strong reflectance. These effects on classification of surface features, measuring vegetation index, and measuring surface reflectance are presented.**

I. Introduction

MEASUREMENTS of the properties of the Earth's surface from satellites, such as Landsats, depend on the optical characteristics of the Earth's atmosphere [12], [14]. Molecular scattering and absorption can be accounted for satisfactorily, but not the optical properties of aerosols for the part of the spectrum dominated by scattering processes as opposed to thermal emission. Kaufman [15] showed how aerosols decrease the apparent spatial resolution. Kaufman and Fraser [17] showed that aerosols modify the apparent spectral characteristics, resulting in loss of classification accuracy. Usually, the aerosol effect on remote sensing is expressed as a function of only the aerosol optical thickness [8], [10], [18]. Aerosol absorption may be another important parameter, since it has been observed to vary several fold [27]. As a result, remote sensing from satellites can be affected significantly by aerosol absorption. Such effects are discussed here.

The absorption properties of atmospheric aerosols are poorly known [1], [9], [26]. Hence, their radiative properties cannot be modeled accurately [3]. Nevertheless, reasonable atmospheric models for calculating the relative effect of aerosol absorption can be specified (Section II). The atmospheric effect on the radiance of scattered sunlight is described in Section III, and the contributions from scattering and absorption are also discussed. Section IV contains examples of the effects on remote sensing of biomass, classification, and measurement of ground reflection. Conclusions are stated in Section V.

Manuscript received December 10, 1984; revised April 25, 1985. This work was supported by the NASA Earth Resource Fundamental Research Program.

R. S. Fraser is with the Laboratory for Atmospheres, NASA Goddard Space Flight Center, Greenbelt, MD 20771.

Y. J. Kaufman is with the University of Maryland, College Park, MD and with the Laboratory for Atmospheres, NASA Goddard Space Flight Center, Greenbelt, MD 20771.

II. Atmospheric Model

The atmospheric model is developed to account for atmospheric radiation effects in the visible and near-infrared spectral bands used for measurements of surface properties from satellites. The scattering characteristics of the standard gases are accounted for. Gaseous absorption is weak and only ozone absorption is included. The aerosol optical properties are computed with application of the Mie theory. Since transmission through atmospheric aerosols frequently can be expressed rather well by a power law for their size distribution [2], [16], such a function is adopted here.

$$\frac{dn}{d \log r} \sim r^{-\nu} \tag{1}$$

where n is the number density of aerosol particles, and r is their radius. Their index of refraction is assumed to be $m = 1.43\text{–}0.0035\ i$, resulting in an albedo of single scattering for the aerosols of $\omega^A = 0.96$. This parameter is explained by realizing that the extinction coefficient (b_e) equals the sum of the scattering (b_s) and absorption (b_a) coefficients. The albedo of single scattering gives the fraction of light that is scattered ($\omega = b_s/b_e$), and the fraction absorbed is $1 - \omega$.

The optical effects caused by aerosol absorption cannot be modeled accurately, since the physical state of the absorbing species is poorly known. The optical properties depend significantly on their state [1]. Aerosol absorption of visible light is attributed predominantly to graphitic carbon generated by combustion processes [6], [20], [23], and [24]. The predominant aerosol absorption is thought to occur at particle sizes smaller than 2 μm [20]; but, because preliminary measurements of the absorption indicate that the absorption coefficient is inversely proportional to wavelength [23], Mie theory indicates that the particles may be smaller than the wavelength [3]. The carbon particles occur in the atmosphere either separately from other particles (the external mode), or mixed with other particles (internal mode). The mode is not known for an entire column of air for satellite measurements. The absorbing particles are modeled here by assuming that they are small compared to the wavelength and in the external mode. Hence, their scattering effects are negligible compared to their absorption effects.

Waggoner *et al.* [27] have reported several values of ω^A measured near the ground in the United States. The values lie in the range of $0.54 \leq \omega^A \leq 0.61$ for urban industrial

areas, $0.73 \leq \omega^A \leq 0.87$ for urban residential areas, and $0.89 \leq \omega^A \leq 1.0$ for nonurban or rural areas. Based on such data and others, Shettle and Fenn [25] suggested values of ω^A, when the relative humidity is 70 percent, of 0.7 for urban aerosols, 0.95 for rural aerosols, and 0.99 for maritime aerosols. Hence, an aerosol albedo of single scattering for a vertical column of the atmosphere can be expected between 0.5 and 1.0. In later discussions the uncertainty in the albedo of single scattering of aerosols for remote sensing in regions outside of urban areas will be assumed as $\Delta\omega^A = 0.1$.

The aerosol optical thickness for the United States at 500 nm varies from a few hundredths to one, or more; and its standard deviation is about one-half of its mean value [7]. The aerosol optical thickness in continental regions varies approximately inversely with wavelength [2].

III. Radiance of Reflected Sunlight

The radiance of the sunlight reflected from the Earth-atmosphere system is computed for several models to show the significance of the two parameters—aerosol optical thickness (τ^A) and albedo of single scattering (ω^A). The radiance L' can be expressed as [11]

$$L'(0, \theta, \phi) = L'_O(0, \theta, \phi) + \frac{\rho F'_D(\tau, \theta_O)\, T(\tau, \theta)}{\pi(1 - \bar{s}(\tau)\rho)} \quad (2)$$

where θ and ϕ are the zenith and azimuthal angles of the direction of propagation of the light; τ is the normal optical thickness of the atmosphere (proportional to aerosol loading); ρ is the hemispherical reflectance of the ground, which reflects light according to Lambert's law; F_D is the total downward flux of light at the ground if $\rho = 0$; T is a transmission function from the ground to the top of the atmosphere for the radiance; and $\bar{s}$ is the reflectance of the atmosphere for isotropic light entering the base of the atmosphere. The first term on the right-hand side of (2) is just the radiance of the atmosphere if the ground were nonreflecting ($\rho = 0$); this term will be called the L_O term. The second term gives the direct and diffuse transmission of light reflected from the ground to a satellite.

Throughout the remainder of this report radiances and fluxes will be normalized to reflectance units. As a result, the normalized radiance L and L_O are related to the absolute spectral radiance L' and L'_O by

$$L = \pi L'/F_O \cos\theta_O$$
$$L_O = \pi L'_O/F_O \cos\theta_O \quad (3)$$

where $F_O \cos\theta_O$ is the solar spectral irradiance incident on a horizontal surface at the top of the atmosphere. The normalized flux is related to the absolute flux F'_D by

$$F_D = F'_D/F_O \cos\theta_O. \quad (4)$$

Equation (2) written in terms of the normalized units becomes

$$L(0, \theta, \phi) = L_O(0, \theta, \phi) + \rho F_D T/(1 - \rho\bar{s}). \quad (5)$$

As an example, if the optical thickness of the atmosphere were $\tau = 0$, then $L_O = 0$, $F_D = 1$, $T = 1$, and the radiance $L(0, \theta, \phi) = \rho$, the surface reflectance. The advantage of using reflectance units is that the difference between L and ρ clearly shows the net atmospheric effect.

The computations are made with a radiative transfer code that was developed originally by Dave and Gazdag [5]. The radiance and scattering phase function were developed in series of cosine functions of the azimuth. As a result, the coefficients of the terms for the radiance are computed as a function of optical parameters and polar angle by an iterative procedure. All orders of multiple scattering are accounted for, but polarization effects are neglected.

The relative significance of the two aerosol parameters (optical thickness and albedo of single scattering) differs for small and large surface reflectance. The essential differences can easily be explained for optically thin atmospheres, which frequently occur during satellite measurements. The L_O term of (5) is dominant when surface reflection is weak. If the solar zenith (θ_O) and viewing angles are not large, then [4]

$$L_O(0, \theta, \phi) = \pi \sec\theta_O \sec\theta \left[\left(\omega \frac{p}{4\pi}\tau\right)^A + \left(\omega \frac{p}{4\pi}\tau\right)^G\right] \quad (6)$$

where the first term in the right-hand side applies to aerosol scattering and the second term to gaseous scattering; p is the scattering phase function, normalized such that its integral over all solid angles equals 4π. The change in radiance due to changes in aerosol optical thickness and albedo of single scattering is

$$\Delta L_O = \pi \sec\theta \sec\theta_O \frac{p^A}{4\pi}(\omega^A \Delta\tau^A + \tau^A \Delta\omega^A).$$

The change in optical thickness implies increasing or decreasing the amount of aerosol, which is partially absorbing in general. The ratio of the last two terms within parenthesis is

$$(\Delta\tau^A/\tau^A)/(\Delta\omega^A/\omega^A). \quad (7)$$

If $\Delta\tau^A/\tau^A = 0.5$ and $\Delta\omega^A/\omega^A = 0.1$, as might be expected for continental regions, then the change in aerosol optical thickness has five times the effect of just the absorption change. The aerosol optical thickness is more important than absorption in accounting for variable aerosol effects over dark surfaces.

The radiance of the Earth-atmosphere system, according to (5), is linearly proportional to the surface reflectance when the term $\bar{s}\rho$ is small, as is usual. When the surface reflectance becomes strong, usually when $\rho > 0.2$, then the second term on the right-hand side of (5) becomes increasingly important. The atmospheric effect for this term depends on atmospheric transmission (F_D and T). An expression for the transmission of sunlight through the atmosphere is [21]

$$F_D = \exp\{-\sec\theta_O\}\{\tau^A[1 - \omega^A(1 - \beta^A)] + \tau^G/2\} \quad (8)$$

where β^A is the fraction of sunlight scattered by the aerosols into the backward hemisphere, which has the sun at its pole. A change in F_D associated with aerosol changes is

$$\frac{\Delta F_D}{F_D} = \sec \theta_O \tau^A \{(1 - \beta^A)\Delta\omega^A - [1 - \omega^A(1 - \beta^A)]\Delta\tau^A/\tau^A\}. \quad (9)$$

The effects of changing aerosol absorption or its optical thickness are about the same, if representative aerosol parameters are used such as $\omega^A = 0.9$, $\Delta\omega^A = 0.1$, $\Delta\tau^A/\tau^A = 0.5$, and $\beta^A \doteq 0.1$, as computed for continental aerosol models. A similar analysis applies to the upward transmission (T). Hence, changes in aerosol absorption and optical thickness have comparable effects on changes of radiance of light reflected from the ground and transmitted through the atmosphere.

Summarizing, the aerosol loading increases the upward radiance through its effect on L_O and decreases the upward radiance through its effect on F_D and T. The aerosol absorption decreases the upward radiance through L_O, F_D, and T. Therefore, while the effect of absorption on the upward radiance increases continuously as a function of the surface reflectance, the effect of the optical thickness is mixed. It increases the radiance for dark surfaces, but the effect is reduced as a function of the surface reflectance, until becoming a decrease for very bright surfaces.

The radiance of models of the Earth-atmosphere is shown as a function of several parameters in Fig. 1. The solar zenith angle is $\theta_O = 40°$. The wavelength is $\lambda = 610$ nm. The gaseous scattering optical thickness is $\tau_s^G = 0.066$; the absorbing gas is ozone and its optical thickness is $\tau_a^G = 0.021$ for a spectral bandwidth of 100 nm. The power for the size distribution is $\nu = 3$. This atmospheric model will be referred to as the standard model. The four curves on each panel of Fig. 1 are labeled with the value of surface reflectance. The difference between this value and the ordinate of the corresponding curve is the change in apparent reflectance caused by the atmosphere. Figs. 1(a) and 1(b) show the radiances for an extreme path length through the atmosphere encountered in current satellite observations. If the aerosol albedo of single scattering is large (Fig. 1(a)), the radiance increases linearly with respect to aerosol total optical thickness, but the rate of increase becomes smaller as the surface reflectance becomes larger. For moderate values of ω^A (Fig. 1(b)) the slopes of the curves decrease and become negative for large surface reflectance. In the latter case, the apparent reflectance decreases markedly with more aerosol. Such an effect would be important in estimating desert reflectance, for example, from satellite observations.

The atmospheric effects with a minimum path length through the atmosphere (nadir viewing) are shown in Fig. 1(c) and 1(d). The light reflected from the ground becomes more important relative to the L_O term of (5). The apparent reflectance of bright surfaces still decreases noticeably with additional amounts of moderately absorbing aerosol.

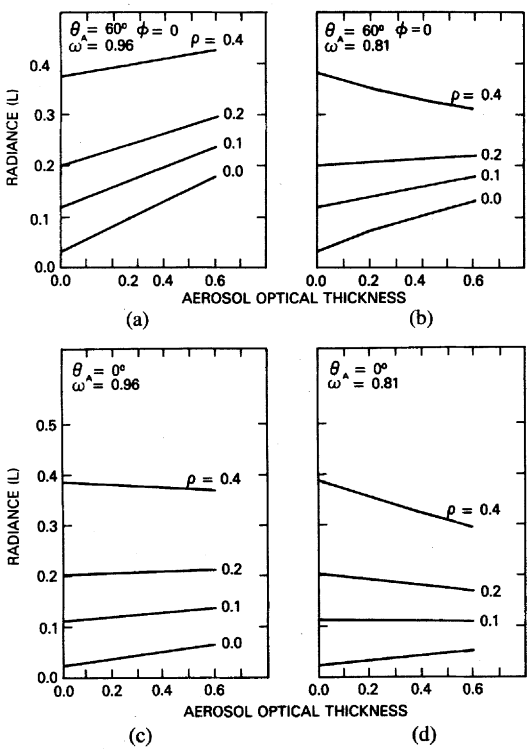

Fig. 1. The radiance (in reflectance units) of light (610 nm) reflected from the Earth-atmosphere system for the standard model as a function of the total aerosol optical thickness and surface reflectance (ρ). (a) and (b) Given for the same zenith (θ) and azimuth (ϕ) angles, but for different albedos of single scattering (ω^A); (c) and (d) for nadir reflectances (θ = 0°). The solar zenith angle $\theta_O = 40°$.

The difference between the radiance above the atmosphere and the surface reflectance is seen from (5) as

$$L - \rho = L_O - \rho(1 - F_D T) \quad (10)$$

where the small term $\rho\bar{s}$ is neglected to simplify this discussion, but is retained in the computations. This difference decreases almost linearly with increasing surface reflectance (Fig. 2). The atmospheric radiance (L_O) is independent of surface reflectance. The next term represents a loss in radiance of the surface because of atmospheric attenuation. The attenuation term is weighted by the surface reflectance ρ. For any one of the two values of albedo of single scattering, the curves for the four values of aerosol optical thickness intersect within the neighborhood of a point. The abscissa of this point will be called the critical surface reflectance (ρ_C). At ρ_C the radiance L may be more or less than the surface reflectance, depending on ω^A.

The significance of ρ_C is that the radiance stays essentially constant as the optical thickness changes. At the critical surface reflectance an increase in aerosol amount results in more backward scattering of direct sunlight, and thus larger L_O; but there is also greater attenuation of light, resulting in smaller flux incident on the ground (F_D) and smaller transmission through the atmosphere (T). Hence, the two terms on the right-hand side of (10) change by the same magnitude, but with the opposite sign. Since the

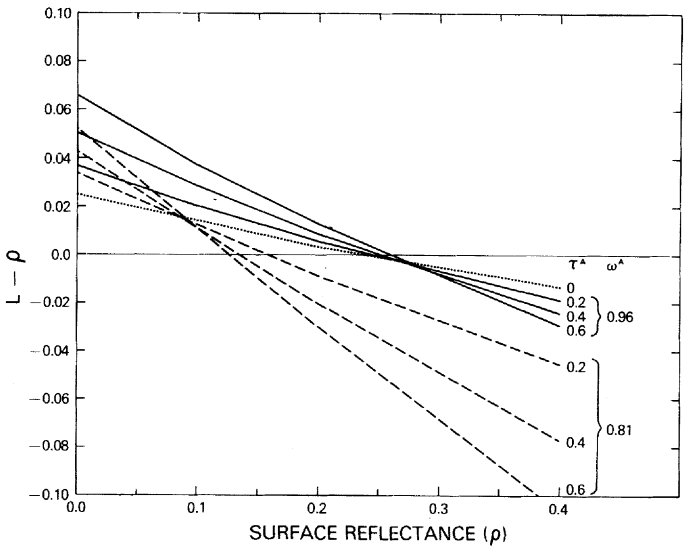

Fig. 2. The radiance of the Earth-atmosphere system minus the surface radiance (in reflectance units) for nadir observation, as a function of the surface reflectance. The total aerosol optical thickness τ^A and the single scattering albedo ω^A are indicated for each line. The solar zenith angle is 40°, the wavelength is 610 nm, and $\nu = 3$.

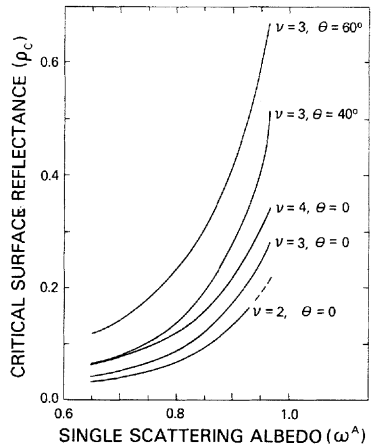

Fig. 3. The critical reflectance ρ_C as a function of the aerosol single scattering albedo (ω^A) for three power law size distributions with exponent ν. The calculations are for wavelength 610 nm and aerosol refractive index $n = 1.43 - 0.0035i$. The observation zenith angle θ is indicated. $\theta_o = 40°$, $\phi = 0°$.

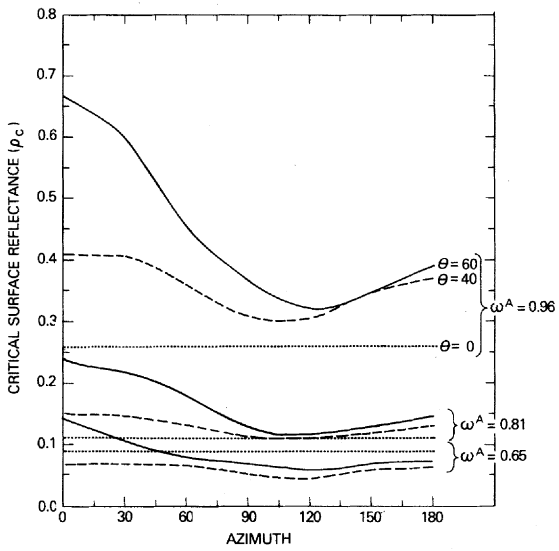

Fig. 4. The critical reflectance as a function of the azimuth between the directions of the solar irradiation and the line-of-sight, for three values of the observation zenith angle θ and three values of the single scattering albedo ω^A · $\nu = 3$ and $\theta_o = 40°$.

change in radiant energy by attenuation is weighted by the surface reflectance, the attenuation becomes stronger (weaker) when the surface reflectance is greater (less) than ρ_C. If the surface reflectance is smaller (larger) than the critical surface reflectance, then the radiance increases (decreases) with increasing optical thickness.

The effect of aerosol absorption on the critical reflectance can be explained by considering an optically thin atmosphere. Substitute the aerosol scattering optical thickness, $\tau_s^A = \omega^A \tau^A$, in (6) for L_O. Then the L_O term does not depend on aerosol absorption. The attenuation term does depend on absorption, however. For example, consider the value of the critical reflectance in Fig. 2 where the L_O and attenuation terms are in balance for $\omega^A = 0.96$. If small absorbing aerosols are added to the atmosphere, ω^A decreases. The L_O term does not change significantly, but the attenuation increases. In order to place less weight on the attenuation term of (10), the critical reflectance decreases until the L_O and attenuation terms compensate for a change in aerosol optical thickness.

The critical reflectance depends on the aerosol scattering phase function (p^A), the length of the path through the atmosphere, and the relative position of the line-of-sight and the sun. Aerosol scattering is such that the relative amount of backward to forward scattering of direct sunlight increases as the power ν increases for a power-law size distribution (1). The L_O term increases with ν; but the attenuation term partially compensates, because less diffuse light is transmitted. The net effect is such that the critical reflectance has to increase to give added weight to the attenuation. Fig. 3 shows that the critical reflectance increases with ν for all three zenith angles. The curve for $\theta = 0$ and $\nu = 3$ corresponds to the case illustrated by Fig. 2.

As the zenith angle (θ) of the light transmitted from the surface to a satellite increases, the optical thickness of the path increases. Both the L_O term and attenuation increase, tending to compensate each other. The scattering angle for direct sunlight changes also, resulting in a change in the scattering phase function. The radiance of scattered light increases more than the attenuation loss, and the critical reflectance has to increase in order for the L_O and attenuation terms to remain in balance.

The critical surface reflectance also depends on the azimuth, since the aerosol scattering phase function depends on the scattering angle. The critical reflectance is given as a function of azimuth for three zenith angles and three ω^A's in Fig. 4. When the zenith angle is fixed, the attenuation term is independent of azimuth. Then ρ_C changes with the L_O term which varies mostly according to the strength of scattering of direct sunlight by the aerosols, since their phase function changes rapidly with respect to scattering angle. Although the strength of scattering by

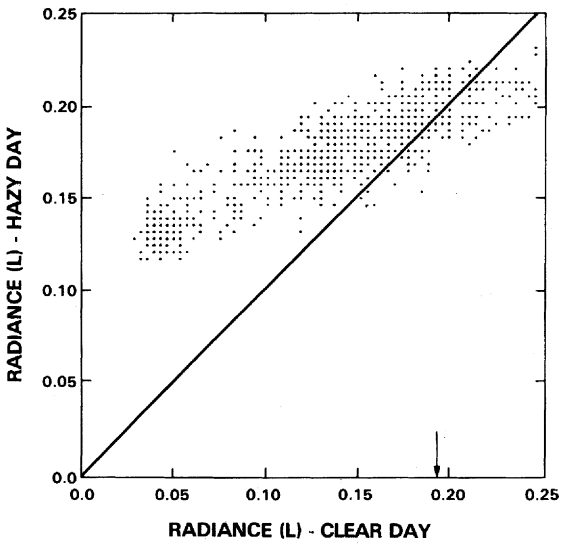

Fig. 5. Scatter diagram of the radiance from a Landsat image on a hazy day as a function of the radiance on a clear day taken over Washington, DC. The arrow indicates the radiance for which no change occurs due to the haziness difference between the clear and the hazy day. The waveband is 700–900 nm; solar zenith angle is 33°.

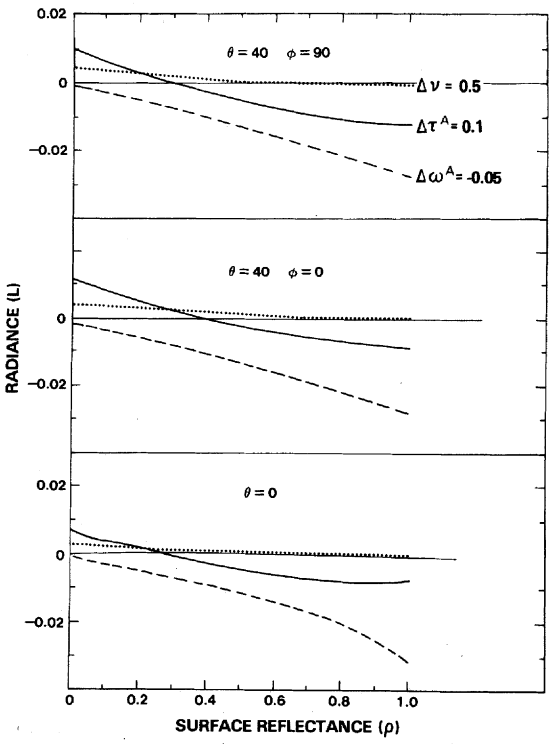

Fig. 6. Changes of the radiance of light (610 nm) reflected from the Earth-atmosphere system as a function of surface reflectance for perturbations of aerosol optical thickness, albedo of single scattering, and size distribution when $\theta_o = 40°$.

the gas is appreciable, its phase function changes slowly with respect to angle. L_O is a maximum in Fig. 4 at the smallest scattering angle, which for example, for $\theta = 60°$ and $\theta_O = 40°$ corresponds to 80° at azimuth 0°; and L_O is a minimum near a scattering angle of 130° or an azimuth between 100° and 120°. The attenuation term is weighted by the critical reflectance, depending on the value of L_O. Also, as seen in Fig. 2, the critical reflectance increases with aerosol albedo of single scattering.

An example of the dependence of the measured atmospheric effect on the surface reflectance is given in Fig. 5. Here the normalized upward radiance for a hazy day (August 2, 1982) was plotted as a function of the upward radiance for a clear day (August 20, 1982). The radiances are derived from the 700–800-nm band of a Landsat image over Washington, DC. The critical reflectance is $\rho_C = 0.18$. With greater amount of haze the radiance increases (decreases), if $\rho < \rho_C (\rho_C < \rho)$.

A quantitative description of the effect of absorption and scattering on the upward radiance can be performed by plotting the radiance response to a perturbation in one of the parameters. Fig. 6 describes results of such perturbation analysis. The unperturbed model is the same model used for Fig. 1(c). The changes in the upward radiance due to perturbations in the optical thickness of $\Delta\tau^A = 0.1$, in the single scattering albedo of $\Delta\omega^A = -0.05$ and in the size distribution $\Delta\nu = 0.5$ [2] are plotted. The plots are for nadir ($\theta = 0°$) and off nadir ($\theta = 40°$) direction of observation.

The changes in radiance can be compared with the specification for Landsat to detect a change of a few thousandths. An increase in the power of the size distribution of $\Delta\nu = 0.5$ results in a small increase in radiance for small surface reflectance, but a negligible change for large reflectance. The aerosol optical thickness perturbation of $\Delta\tau^A = 0.1$ results in significant increase (decrease) in radiance for small (high) surface reflectance. The change in albedo of single scattering results in the largest effect, at least for the assumed perturbation ($\Delta\omega^A = -0.05$).

For a given perturbation in the optical thickness $\Delta\tau^A$, there always is a perturbation in the single scattering albedo $\Delta\omega^A$ that for a specific value of the surface reflectance results in the same change in the radiance. Such results can be represented by a phase diagram given in Fig. 7, which shows the surface reflectance where aerosol absorption ($1 - \omega^A$) or optical thickness is the more significant parameter associated with changes of the nadir radiance of the Earth-atmosphere system. The reflectance of the surface of the Earth ranges over nearly the entire range of the abscissa, and the ordinate covers only part of the range of aerosol absorption. The aerosol scattering optical thickness of the reference model is perturbed by increasing it 0.1. The ordinate gives the perturbation in aerosol absorption. Since the critical reflectance $\rho_C = 0.27$ in this example, the change in radiance with just the optical thickness is positive (negative) for surface reflectance less (greater) than ρ_C. Along the continuous line there is no change in radiance, since a perturbation by the aerosol absorption results in a complete compensation for the radiance change resulting from the optical thickness perturbation. The plus and minus signs indicate the sign of the net radiance change in the shaded regions. The absorption and optical thickness perturbations result in radiance changes of the same value along the dashed line. The optical thickness causes the larger radiance change in the hatched region. The major significance of this diagram is

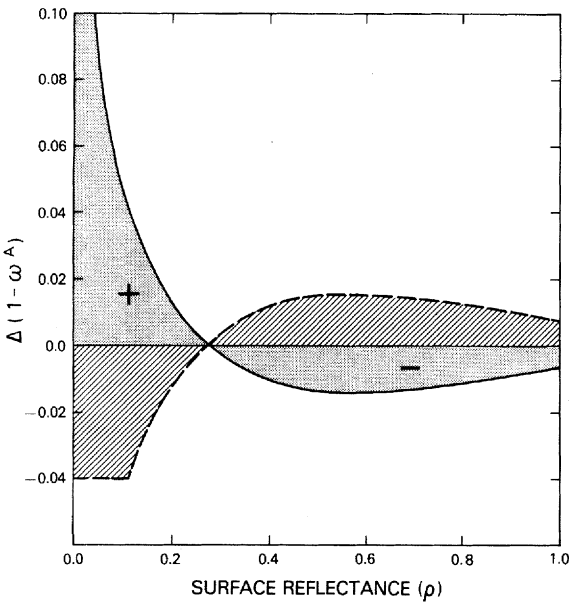

Fig. 7. Relative changes of nadir radiance of the Earth-atmosphere system due to perturbations of aerosol optical thickness ($\Delta\tau^A = 0.10$) and absorption (ordinate) as a function of surface reflectance. $\theta_o = 40°$ and $\lambda = 610$ nm. For the unperturbed model $\tau^A = 0.3$, $\omega^A = 0.96$.

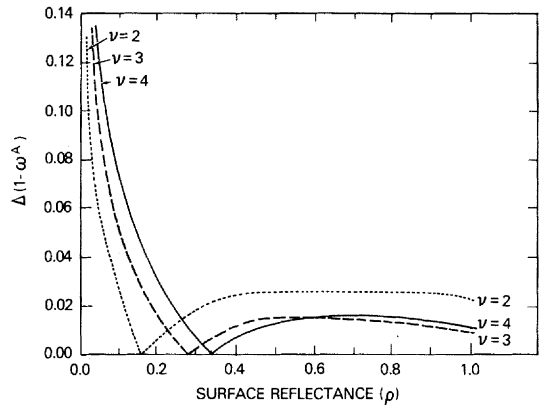

Fig. 8. Same as in Fig. 7, but for three power law size distributions with exponent ν.

that aerosol absorption is more important than optical thickness in many remote sensing situations, which is the region that is not shaded or hatched in Fig. 7. The size of the unshaded areas depends on the aerosol scattering phase function, and, therefore, on the aerosol size distribution. In Fig. 8 the upper half of the diagram of Fig. 7 is reproduced for $\nu = 2$, 3, and 4. A higher value of ν means that the size distribution has more small particles with strong backward scattering. As a result, the critical reflectance increases, shifting with it the whole equal response curve.

IV. Applications

A. Satellite Measurement of Biomass

We shall use the example of satellite measurements of biomass to show the relative effects of aerosol absorption and optical thickness. Such measurements are commonly made by comparing the contrast in radiances of the near infrared and red spectra, since green biomass, such as tree leaves, has strong reflectance in the near-infrared spectrum, but weak for red light. The contrast is expressible as a normalized difference (ND)

$$\mathrm{ND} = \frac{1 - \gamma}{1 + \gamma}$$

$$\gamma = L(660\text{ nm})/L(820\text{ nm}). \qquad (11)$$

Holben and Fraser [13] found that the ND depended significantly on the aerosol optical thickness, but the absorption effect was not studied.

The relative effects of aerosol absorption and optical thickness are computed for models consisting of the four surface types given in Table I, and the four atmospheric models consisting of the standard scattering and absorbing gases plus aerosols whose characteristics are given in Table II. The aerosol optical thickness properties are based on summer observations at Washington, DC. [16]. Values less than 0.3 were measured 30 percent of the time, and values exceeding 0.86 were measured 15 percent of the time. Peterson *et al.* [22] found similar values for North Carolina. Therefore, models 1 and 2 represent low haziness and models 3 and 4 represent hazy conditions. The absorption is weak for models 1 and 3, but moderate for models 2 and 4.

The radiances of the Earth-atmosphere models consisting of dense alfalfa and the four aerosol models of Table II are plotted in Fig. 9 for two viewing directions. For either of the two directions, the spread of the four points indicates the problem caused by the atmosphere, when surface classifications are made by means of clustering

TABLE I
Cover Type, Green Biomass Levels, and Measured Reflectance at the Surface [19]

Cover Type	Green Biomass (g/m^2)	Reflectance at Surface		ND
		Red	NIR	
Clean Water	0.	.00	.00	—
Bare Soil	0.	.20	.25	0.11
Alfalfa Low Biomass Level	260.	.10	.20	0.33
Alfalfa Medium Biomass Level	660.	.05	.25	0.67
Alfalfa High Biomass Level	1400.	.03	.40	0.86

TABLE II
Aerosol Models Associated with Simulation of Biomass Observations. The Power of the Size Distribution is 3.7 (The symbol for aerosol scattering optical thickness is τ_S^A.)

	Average τ_S^A				Large τ_S^A			
	1		2		3		4	
	Weak Absorption		Moderate Absorption		Weak Absorption		Moderate Absorption	
Parameter	660	820	660	820	660	820	660	820
τ_S^A	0.287	0.200	0.287	0.200	0.861	0.600	0.861	0.600
total optical thickness	0.366	0.276	0.395	0.296	0.961	0.692	1.049	0.753
ω^A	0.964	0.960	0.878	0.876	0.962	0.960	0.878	0.876

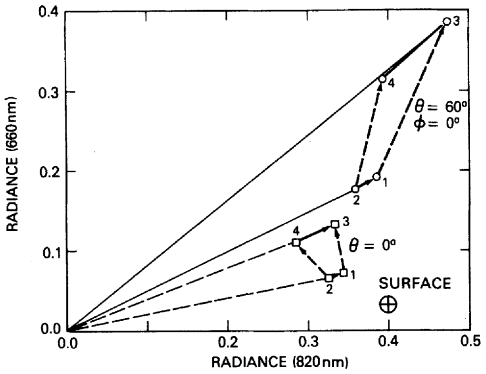

Fig. 9. Radiance of models of the Earth-atmosphere system. The surface consists of dense alfalfa (high biomass density) of Table I. The numbers beside the plotted points refer to the aerosol models of Table II. θ_o = 50°.

techniques. Whenever gradients in the aerosol optical properties occur, the points are dispersed.

The ratio γ in (11) for the measure of biomass equals the slope of a line through a radiance point and the coordinate origin of Fig. 9. If the atmospheric properties vary in such a way that the slope of a line through the observation point does not change, then the ND is independent of the atmospheric properties. When the aerosol albedo of single scattering increases in the transition from point 2 to 1, or 4 to 3, the slope changes only slightly, because the relative change in radiance is nearly the same for both spectral bands. Hence, changes in aerosol absorption have a weak effect on the ND. On the other hand, the ratio γ changes significantly as the aerosol optical thickness increases from 1 to 3 or 2 to 4. More generally, this diagram implies that measures of contrast between bright and dark surface, such as given by (11), are insensitive to aerosol absorption, but decrease with increase in aerosol optical thickness.

B. Classification

The atmospheric effect on classification and the role of ω^A, and τ^A in it, can be described with the aid of Figs. 9–11. As was mentioned before, the spread between the values associated with the four atmospheric models in Fig. 9 indicates the atmospheric effect on classification of surface objects by means of clustering. To illustrate the effect, the nadir radiances for the four atmospheric models and the five land covers given in Table I are tabulated in Table III together with the resulting vegetation index ND. The radiances are plotted in Fig. 10. For a given atmospheric model the classes are well separated. Once all the atmospheric models are introduced, as in Fig. 10, the classes are less separable. For example, bare soil for high absorption and both small and large amounts of haze (models 2 and 4) is located very close to alfalfa with low biomass for a hazy atmosphere with low absorption (model 3). Therefore, in this simplified two-band classification, uncertainty in the atmospheric absorption brings the two classes to a separation of only $\Delta L = 0.02$.

The effect of aerosol absorption on the radiance of dense alfalfa is shown as function of wavelength in Fig. 11. It is

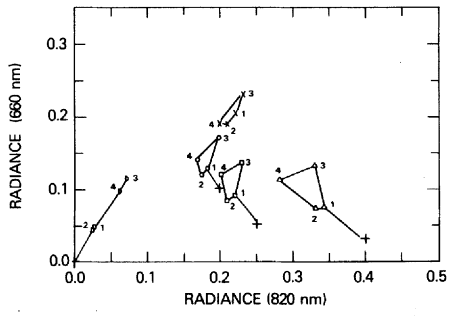

Fig. 10. The radiances in two spectral bands of the Earth-atmosphere for the surface models given in Table I and atmospheric models in Table II. θ = 0°, θ_o = 50°. + shows surface reflectance; × shows bare soil; ○, □, and △ alfalfa: low, medium, and high biomass, respectively; ●, water.

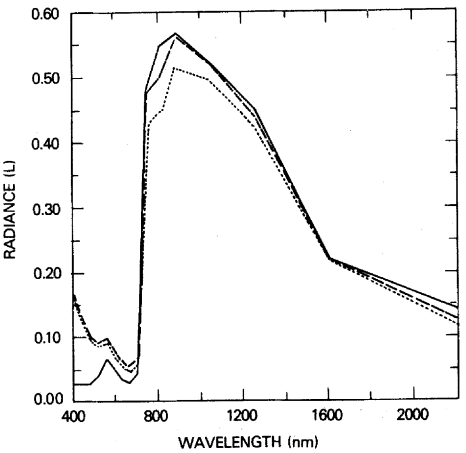

Fig. 11. The surface reflectance for dense alfalfa (solid line) [28], the upward radiance (dashed line) at nadir for relatively clear conditions (aerosol optical thickness is 0.25 at 560 nm) and low absorption $\omega^A \cong 0.96$, and the radiance for the same optical thicknesses, but moderate absorption $\omega^A \cong 0.81$ (dotted line). The solar zenith angle is 30°.

TABLE III
THE UPWARD RADIANCE FROM THE NADIR AND THE VEGETATION INDEX ND AT THE TOP OF THE ATMOSPHERE FOR THE FOUR LAND COVERS OF TABLE I AND FOR THE FOUR ATMOSPHERIC MODELS OF TABLE II

	λ	RADIANCE (L) Model 1	Model 2	Model 3	Model 4	ND M1	M2	M3	M4
Bare soil	660	.205	.191	.233	.188	.042	.053	−.005	.026
	820	.222	.211	.230	.197				
Alfalfa Low biomass	660	.126	.118	.173	.142	.18	.19	.064	.087
	820	.183	.174	.197	.169				
Alfalfa Medium biomass	660	.087	.082	.144	.120	.44	.44	.23	.24
	820	.223	.211	.230	.197				
Alfalfa High biomass	660	.072	.068	.132	.111	.65	.65	.43	.44
	820	.344	.326	.332	.282				
Water	660	.048	.046	.115	.098	−0.33	−0.28	−0.24	−0.22
	820	.024	.026	.071	.063				

seen that for short wavelengths ($\lambda < 750$ nm) the two atmospheric models (dotted and dashed lines) give similar results. This is due to the low surface reflectance at these wavelengths. For longer wavelengths ($0.75 < \lambda < 1.4$ nm) the atmospheric effect for the low absorbing model is very small, while strong reduction in the radiances is found for the more absorbing model.

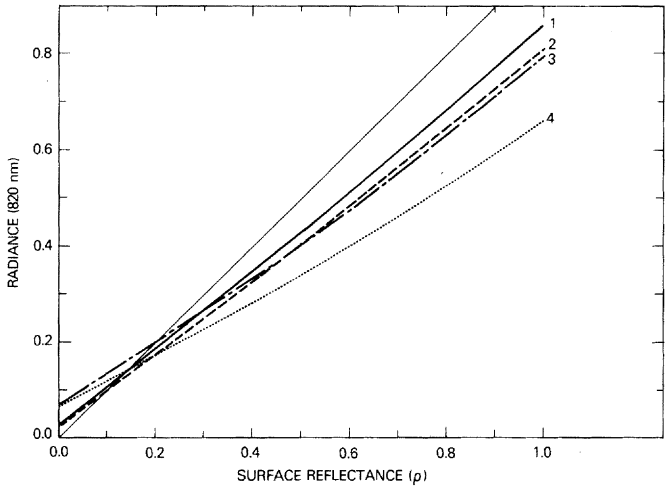

Fig. 12. The upward radiance as a function of the surface reflectance for four atmospheric models of Table II. The thin solid line is for no atmosphere. $\theta = 0°$ and $\theta_o = 50°$.

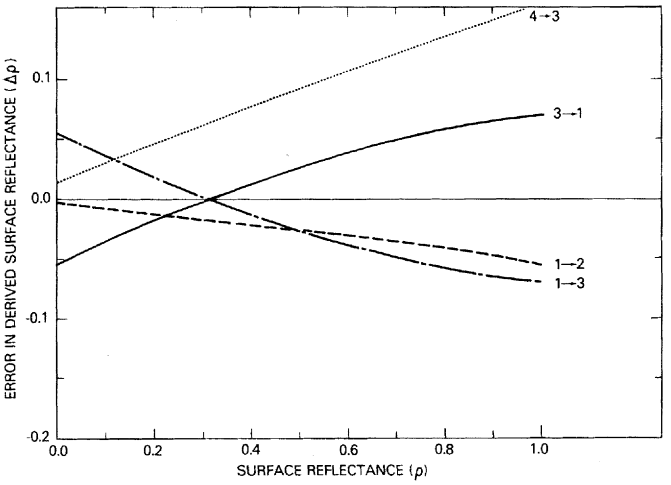

Fig. 13. The error in the remotely sensed surface reflectance as a function of the surface reflectance due to an error in the atmospheric model. The first and second numbers at the end of a curve refer to the assumed and true models, respectively.

C. Surface Reflectance

Remote measurement of surface reflectance is also strongly affected by the atmospheric aerosols. The radiance is given as a function of surface reflectance in Fig. 12 for the atmospheric models of Table II. The radiance is much less than the surface value for all models with high surface reflectance. These radiances are used in Fig. 13 to derive the error in the remotely sensed surface reflectance due to a wrong assumption of the atmospheric model. The error in the remotely secured surface reflectance is plotted as a function of the surface reflectance itself (Fig. 13). For example, the (1 → 2) curve represents the error due to an assumption that the atmosphere has a small optical thickness and absorption (model 1) while the true atmosphere has higher absorption (model 2).

The 1 → 3 curve gives the error in derived surface reflectance by assuming that the aerosol optical thickness is too small by 0.4. At the point where the surface reflectance is 0.32 the error vanishes, since the radiance is independent of the amount of aerosol for $\omega^A = 0.96$ and the geometry of this example. If on the other hand the albedo of single scattering is underestimated for the hazy atmosphere (4 → 3), large reflectance errors result. In desert regions where the surface reflectance is 0.40, the derived surface reflectance would be 0.47. The desert albedo for the entire solar spectrum would tend to be overestimated, if the albedo of single scattering were underestimated since the error is positive, at least for $\Delta\omega^A = -0.15$.

V. Conclusion

Satellite measurements of properties of the Earth's surface depend on aerosol absorption. The significance of this effect on analyses of satellite observations cannot be established without additional information on the optical properties of absorbing aerosols, which depend on the aerosol albedo of single scattering and its scattering phase function. These properties are required for essentially the lower part of the troposphere, which contains a large fraction of the aerosol. Only a few measurements of the aerosol albedo of single scattering have been made, mostly near the surface, however. The aerosol optical properties cannot be extrapolated upward from such data, since they depend on whether the absorbing particles are internal or external to the dominant nonabsorbing particles. Both states occur, but investigations concerning this are incomplete. Investigations have commenced, however, to measure the important optical properties of absorbing aerosols that are relevant properties for remote sensing.

Acknowledgment

The authors are grateful to S. Matoo for performing the computations.

References

[1] T. P. Ackerman and O. B. Toon, "Absorption of visible radiation in atmosphere containing mixtures of absorbing and nonabsorbing particles," *Appl. Opt.*, vol. 20, pp. 3661-3668, 1981.

[2] A. Angstrom, "The parameters of atmospheric turbidity," *Tellus*, vol. 16, pp. 64-75, 1964.

[3] C. F. Bohren and D. R. Huffman, *Absorption and Scattering of Light by Small Particles*. New York: Wiley, 1983, pp. 130-136.

[4] S. Chandrasekhar, *Radiative Transfer*. New York: Dover, p. 273, 1960.

[5] J. V. Dave and J. Gazdag, "A modified Fourier transform method for multiple scattering calculations in a plane-parallel atmosphere," *Appl. Opt.*, vol. 9, pp. 1457-1466, 1970.

[6] J. D. Edwards, J. A. Ogren, R. E. Weiss, and R. J. Charlson: "Particulate air pollutants: A comparison of British 'Smoke' and elemental carbon concentration," *Atmos. Environ.*, vol. 17, pp. 2337-2341, 1983.

[7] E. C. Flowers, R. A. McCormick, and K. R. Kuris, "Atmospheric turbidity over the United States," *J. Appl. Meterol.*, vol. 8, pp. 955-962, 1969.

[8] R. S. Fraser, O. P. Bahethi, and A. H. Al-Abbas, "The effect of the atmosphere on classification of satellite observations to identify surface features," *Remote Sensing Environ.*, vol. 6, pp. 229-250, 1977.

[9] H. E. Gerber, and E. E. Hindman, Ed., *Light Absorption by Aerosol Particles*. Spectrum Press, 1982.

[10] H. R. Gordon, D. K. Clark, J. W. Brown, O. B. Brown, R. H. Evans, and W. W. Broenkow, "Phytoplankton pigment concentrations in the Middle Atlantic Bight: Comparison of ship determinations and CZCS estimates," *Appl. Opt.*, vol. 22, pp. 20-36, 1983.

[11] J. E. Hansen and L. D. Travis, "Light scattering in planetary atmospheres," *Space Sci. Rev.*, vol. 16, pp. 527-610, 1974.

[12] B. M. Herman and S. R. Browning, "The effect of aerosols on the Earth-atmosphere albedo," *J. Atmos. Sci.*, vol. 32, pp. 1430–1445, 1975.
[13] B. Holben and R. S. Fraser, "Red and near-infrared sensor response to off-nadir viewing," *Int. J. Remote Sensing*, vol. 5, pp. 145–160, 1984.
[14] R. B. Horvath, J. G. Polcyn, and C. Fabian, "Effects of atmospheric path on airborne multispectral sensors," *Remote Sensing Environ.*, vol. 1, pp. 203–215, 1970.
[15] Y. J. Kaufman "Atmospheric effect on spatial resolution of surface imagery," *Appl. Opt.*, vol. 23, pp. 3400–3408, 1984.
[16] Y. J. Kaufman and R. S. Fraser, "Light extinction by aerosols during summer air pollution," *J. Climate Appl. Meterol.*, vol. 22, pp. 1694–1706, 1983.
[17] Y. J. Kaufman and R. S. Fraser, "Atmospheric effect on classification of finite fields," *Remote Sensing Environ.*, vol. 15, pp. 95–118, 1984.
[18] Y. Kawata, Y. Haba, T. Kusaka, Y. Terashita, and S. Ueno, "Atmospheric effects and their correction in airborne sensor and Landsat MSS data," in *Proc. 12th Int. Symp. Remote Sensing Environ, ERIM* (Ann Arbor, MI), 1978.
[19] J. A. Kirchner, D. S. Kimes, and J. E. McMurtrey, III, "Variation of directional reflectance factors with structural changes of a developing alfalfa canopy," *Appl. Opt.*, vol. 21, pp. 3766–3774, 1982.
[20] J. P. Lodge, Jr., A. P. Waggoner, D. T. Klodt, and C. N. Crain: "Non-health effects of airborne particulate matter," *Atmos. Environ.*, vol. 15, pp. 431–482, 1981.
[21] W. E. Meador and W. R. Weaver, "Two-stream approximation to radiative transfer in planetary atmospheres: A unified description of existing methods and a new improvement," *J. Atmos. Sci.*, vol. 37, pp. 630–643, 1980.
[22] J. T. Peterson, E. C. Flowers, G. J. Berri, C. L. Reynolds, and J. H. Rudisill, "Atmospheric turbidity over central North Carolina," *J. Appl. Meterol.*, vol. 20, pp. 229–241, 1981.
[23] H. Rosen and T. Novakov, "Soot in the Artic," *Atmos. Environ.*, vol. 15, pp. 1371–1374, 1981.
[24] G. V. Rosenberg, "On the nature of aerosol absorption in the short-wave region of the spectrum," Izv., *Atmos. Ocean. Phys.*, vol. 15, pp. 898–906, 1979.
[25] E. P. Shettle and R. W. Fenn, "Models for the aerosols of the lower atmosphere and the effects of humidity variations on their optical properties," Air Force Geophys. Lab., Hanscom AFB, MA, 1979.
[26] S. Twomey and D. R. Huffman, *Workshop Review. Light Absorption by Aerosol Particles*, H. E. Gerber and E. E. Hindman, Eds. Spectrum Press, 1982, pp. 395–408.
[27] A. P. Waggoner, R. E. Weiss, N. C. Ahlquist, D. S. Covert, S. Will, and R. J. Charlson, "Optical characteristics of atmospheric aerosols," *Atmos. Environ.*, vol. 15, pp. 1981–1909, 1981.
[28] D. Deering, private communication.

*

Robert S. Fraser received the Ph.D. degree in meteorology from the University of California at Los Angeles in 1960.

He served as a Meteorologist in the U.S. Air Corps, retiring as a Captain in 1946. He was employed at TRW Systems for 12 years doing applied researach on atmospheric effects on the guidance of intercontinental ballistic missiles, reconnaissance from satellites, and remote sensing. He joined the NASA Goddard Space Flight Center in 1971, where he has concentrated on measuring atmospheric properties from satellites and also on atmospheric effects on remote sensing.

*

Yoram J. Kaufman received the B.Sc. and M.Sc. degrees in physics from the Technion-Israel Institute of Technology, Israel, in 1972 and 1974, respectively, and the Ph.D. degree from Tel-Aviv University in 1979.

He is currently working at the Department of Meteorology, University of Maryland, and at the NASA Goddard Space Flight Center. He conducts both theoretical and experimental research on the atmospheric effect on remote sensing of the Earth's surface, as well as research on the aerosol characteristics from ground-based, aircraft, and satellite observations. He developed a three-dimensional radiative transfer model that is applied to remove the atmospheric effect from satellite images of the Earth. The results of the research are also applied to studies of the transport of regional air pollution aerosol, forest-fire smoke, and Saharan dust.